

Determination of epitaxial overlayer structures from high-energy electron scattering and diffraction

E. L. Bullock and C. S. Fadley

Department of Chemistry, University of Hawaii, Honolulu, Hawaii 96822

(Received 27 August 1984)

Angle-resolved x-ray photoelectron and Auger data recently obtained by Egelhoff from epitaxially grown Cu on a Ni(001) substrate are analyzed with the use of a single-scattering cluster model. The intensity variations as a function of polar angle are well reproduced by this model, and it permits an analysis of the single-atom origins of the observed peaks. Forward scattering from the first few spheres of neighbors is found to dominate at energies ≥ 900 eV, thus providing detailed information on the early stages of epitaxial growth.

The epitaxial growth of one substance on the ordered surface of another is a subject of high current interest in many fields. In this Rapid Communication we discuss a novel application of high-energy photoelectron and Auger scattering and diffraction to the study of the atomic structure of epitaxial overlayers. Several prior studies have shown that x-ray photoelectron scattering and diffraction (XPD) at ≥ 1 keV can provide several types of information concerning adsorbate and substrate atomic structures, and that the analysis of such data can often be considerably simplified because of the dominance of forward-peaked elastic scattering and the applicability of a simple single-scattering cluster (SSC) model.^{1,2} In particular, forward scattering can provide very direct information on the orientations of molecular adsorbates.^{1,2} More recently, Egelhoff^{3,4} has qualitatively discussed the effects of forward scattering in experimental data for epitaxial Cu on Ni(001), and pointed out the potential utility of such measurements for studying such overlayers. We here present the first SSC analysis of this type of data, including the detailed atomic origins of different peaks observed, and discuss the utility of such high-energy diffraction as a sensitive structural tool for studying the early stages of epitaxial growth.

In the experimental study cited above,^{3,4} measurements were made of the Mg $K\alpha$ -excited Cu $2p_{3/2}$ (317 eV kinetic energy) and Cu $3p$ (1173 eV) photoelectron intensities and the Cu $2p3d3d$ (917 eV) Auger intensity as functions of polar angle for Cu grown epitaxially on a Ni(001) surface. Data were taken for Cu thicknesses of between 0.6 and 14 monolayers (ML). Figure 1 schematically shows the experimental geometry, with several directions of possible simple forward scattering noted. The most detailed experimental data for the 917-eV Auger case are reproduced as solid curves in Fig. 2.

Using these data and the fact that Cu is thought to deposit pseudomorphically layer by layer rather than by island formation,⁵ Egelhoff^{3,4} has postulated that simple forward scattering from atoms lying along the emitter-detector direction is responsible for the structure observed in the curves. For instance, at 1 ML or less (cf. Fig. 1), no forward-scattering effects should be observed according to this model (except for scattering near $\theta = 0^\circ$ that is experimentally very difficult to observe) and the spectra should mimic the rather flat surface-layer instrument response function.² At 2 ML, however, the fcc structure permits forward scattering of electrons emitted from second-layer atoms by

overlying atoms in the first layer that might produce two diffraction peaks: one at 45° and one at 18.4° with respect to the surface (cf. Fig. 1). Also shown in Fig. 1 are forward-scattering peaks which might be expected to appear at higher coverages. At 3 ML, peaks at 90° and 26.6° could appear and at 4 ML one at 71.6° could appear. However, the events shown at 18.4° , 26.6° , 63.4° , and 71.6° are due to scattering from atoms farther away from the emitter, and they are thus qualitatively expected to be of lesser importance. Notice also that forward scattering at 45° should be reinforced for each added layer, thus producing a large intensity maximum in this direction; by contrast, scattering at 90° is reinforced only by every other added layer. Comparing experimental peak positions and the thickness at which they appear with the directions noted at the bottom of Fig. 2 suggests that this simple picture has some validity in describing Cu growth on Ni(001). For example, the 45° and 90° peaks show onsets at the expected coverages and at the correct positions.

In order to more quantitatively analyze both the Auger and photoelectron data, we have carried out a series of SSC

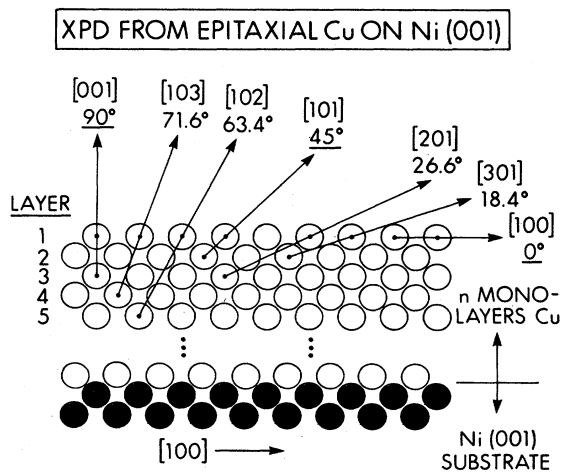


FIG. 1. Structure of ideally epitaxial Cu on Ni(001), with various simple forward-scattering events from overlying Cu atoms that may produce peaks in emission at particular angles also indicated.

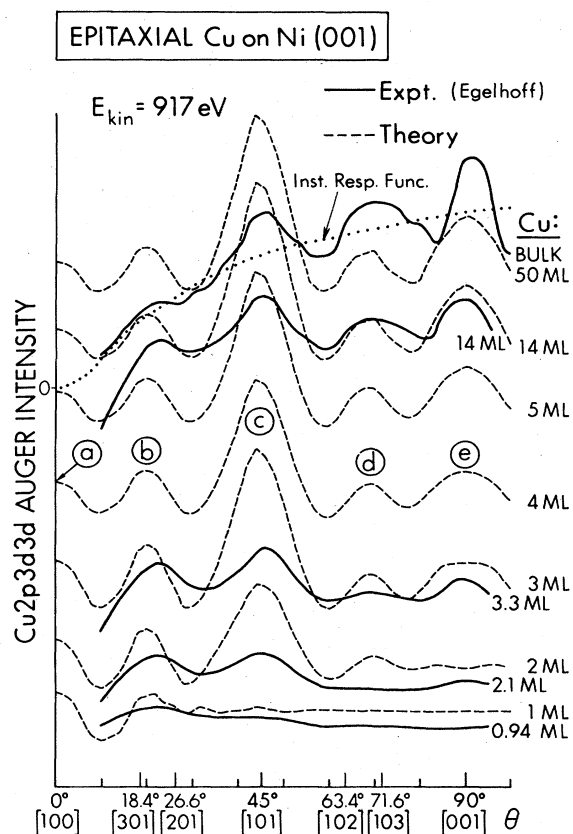


FIG. 2. Polar-angle scans of Cu $2p3d3d$ Auger emission at 917 eV for various coverages of Cu on Ni(001). The azimuthal plane of the scan is indicated at the base of the figure. The solid lines are from the experimental work of Egelhoff (Refs. 4 and 5); the dashed lines, with peaks labeled (a)–(e), are the result of our SSC calculations. The dotted curve shows the approximate experimental instrument response function for a bulk sample. The directions and angles associated with various simple forward-scattering events are indicated on the θ axis.

calculations. The basic assumptions, equations, and input parameters used in these calculations are discussed in detail elsewhere.^{1,2} Photoelectron excitation amplitudes were taken to vary as $\hat{\epsilon} \cdot \hat{k}$, where $\hat{\epsilon}$ is the polarization direction and \hat{k} the emission direction; this is exact for s -level emission and also has been shown to be a fully adequate approximation for the cases of p -level emission studied here.^{1,2} In Auger emission for which all three subshells involved are filled—the case of relevance here—an isotropic excitation amplitude has been used, although prior work^{2,6} indicates that the difference between using that and $\hat{\epsilon} \cdot \hat{k}$ in the SSC calculations is very slight due to the dominance of forward scattering. Both elastic scattering amplitudes and inelastic scattering mean free paths were chosen to be $\frac{1}{2}$ of their usual values; these empirical adjustments have been shown to provide better agreement with experiment in prior studies,^{1,2,7–9} although the predicted curves for the present case are not particularly sensitive to these choices. The calculations were angle averaged over an acceptance cone of $\pm 2.3^\circ$ to simulate experimental angular resolution. Fully converged results were obtained with a cluster size of ~ 140 atoms per layer.

The results of calculations for the 917-eV Auger case are shown along with the available experimental data^{3,4} in Fig. 2. When comparing experiment and theory it is important to note that the slope of the instrument response function (as shown in Fig. 2) at lower electron-emission angles may affect the agreement in this region, and may be responsible for small discrepancies in the position of peak (b), as well as in the relative intensities of peaks (c) and (e). All experimental spectra go to zero at $\theta = 0^\circ$ as a result of this function, whereas the theoretical curves have an approximately constant average value. Thus, the theoretical peak labeled (a) will not be observable.

Considering the Auger results in detail, we see, in general, excellent agreement as to the positions and relative intensities of various features, including the nature of their evolution with increasing Cu thickness. The relatively featureless experimental curve for 0.94 ML agrees well with the flat theory curve for 1 ML; a weak feature in theory at $\theta = 20^\circ$ also appears to be present in experiment. The 2.1 ML experimental curve also agrees well with 2 ML theory as to the two strong features (b) and (c) at 21° and 45° , respectively. The 3.3 ML experimental curve also agrees well with theory as to all four peaks (b)–(e) occurring at 20° , 45° , 69° , and 90° . The presence of a weak peak at 90° in the 2.1 ML experimental data also suggests a small fraction of 3 ML islands when compared to both experiment and theory for 3 ML. The thicker 14 ML and bulk curves also show excellent agreement, although the bulk experimental curve exhibits somewhat more fine structure than theory, perhaps due to too much angular averaging in the theoretical calculation. Note also that the theoretical curves converge to a very nearly constant form by about 4–5 ML thickness. Only very subtle changes in relative intensity or fine structure occur as layers are added beyond 5 ML, although coverages of 50 ML were used to ensure complete depth convergence for comparisons to bulk experimental spectra.

Although experimental data are available at 1173 eV only for 0.6 ML, 2 ML, and bulk,^{3,4} a comparison analogous to that of Fig. 2 shows that the agreement between experiment and theory is again excellent for both 2 ML and bulk. The experimental curve for 0.6 ML shows only very weak structure, in qualitative agreement with the very flat theoretical prediction for 1 ML; however, weak features observed at $\theta = 20^\circ$, 45° , and 72° very close to those labeled (b)–(d) in Fig. 1 suggest the presence of a certain fraction of 2 ML islands. Thus, the Auger experimental data of Fig. 2 at 0.94 ML seem to be for an overlayer that is more purely 1 ML than the photoelectron data. The very close similarity found in both the 2 ML and bulk experimental curves between the Auger and photoelectron data also confirms the relative insensitivity of these measurements to the exact form of the primary Auger or photoelectron excitation amplitude.

In order to study the origin of the observed peaks in more detail, a series of calculations were carried out to determine the effects of various individual scatterers. This was done by considering either clusters made up simply of an emitter and one scatterer or clusters in which particular scatterers were removed from a full n -layer system. The results of these calculations for the 1173-eV photoelectron case are shown in Fig. 3. (Identical results are found for 917-eV Auger emission.) The top curve indicates that peak (a) in the theory is the result of forward scattering from the nearest neighbor Cu in the first layer. Note also that

scattering from this atom produces a sizable first-order diffraction peak^{1,2} at the position of peak (b). A comparison with the second curve, in which the full 1 ML calculation is reproduced, shows that other 1 ML atoms contribute only very slightly to the intensity of peaks (a) and (b). The third through sixth curves relate to emission from 2 ML, and a summation of independent emission from typical atoms in each of the two layers must therefore be considered. Removing a first-layer atom that can scatter at 45° from a second-layer emitter in a 2 ML cluster yields a curve very much like 1 ML; this confirms the importance of nearest-neighbor scattering. Removing the more distant 18.4° atom from the 2 ML cluster results in the fourth curve in Fig. 3. Comparing this with the full 2 ML calculation (fifth curve) shows that this 18.4° atom does contribute to peak (b), but in a less significant way involving only ~30%–40% of its total intensity. The analysis of peak (c) is more straightforward. This peak turns on dramatically at 2 ML, and, when the 45° atom thought responsible for it is removed from the cluster, this peak disappears completely, as shown in the

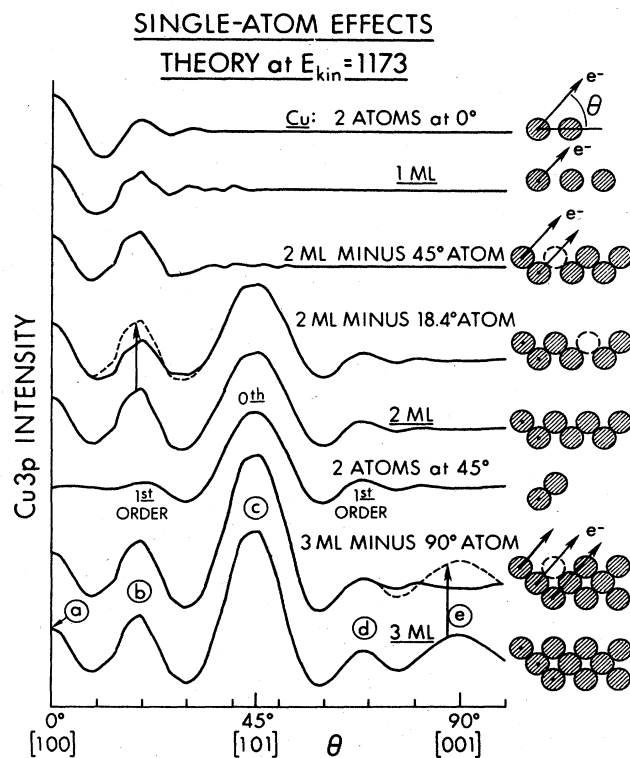


FIG. 3. Theoretical polar-scan curves for $E_{kin} = 1173$ eV and various clusters chosen to illustrate the effects of various single atoms on the full-cluster diffraction patterns. From top to bottom the curves represent (1) a two-atom cluster which includes only the emitter and the horizontal atomic scatterer at $\theta = 0^\circ$ (cf. Fig. 1), (2) a full cluster of 1 ML, (3) a full cluster of 2 ML minus the scattering atom at 45° with respect to a second-layer emitter, (4) a full cluster of 2 ML minus the 18.4° atom, where the dotted line indicates the full 2 ML cluster and thus measures the effect of this atom, (5) a full cluster of 2 ML, (6) a two-atom cluster which includes only the emitter and the 45° scattering atom, (7) a full cluster of 3 ML minus the 90° atom, where the dashed line indicates the full 3 ML cluster, and (8) a full cluster of 3 ML. Sketches to the right indicate the cluster used for each calculation; the independent emitters in each layer are shown by arrows.

third curve of Fig. 3. The results of a calculation which includes in the cluster only a second-layer emitter and the 45° atom (sixth curve) show the strong peak at 45° and smaller first-order peaks to either side at $\theta \approx 22^\circ$ and 67° . Thus, there are first-order diffraction contributions to both peaks (b) and (d). If simple "zeroth-order" forward scattering^{1,2} from overlying Cu atoms were the major cause of peaks in these spectra, peak (d) would occur only at 4 ML (cf. Fig. 1). From Fig. 2, however, peak (d) is fully developed by about the third layer in the calculations, indicating that simple forward scattering along [103] and [102] plays a very minor role in producing this peak. Instead, an examination of the last three curves in Fig. 3 shows that peak (d) is an approximately equal mixture of two first-order diffraction peaks: one from the 45° atom and one from the 90° atom. The latter contribution is clear from the disappearance of the right minimum of peak (d) when the 90° atom is removed from the cluster; the 2 ML and 3 ML minus 90° atom curves are thus also very nearly identical for $\theta \geq 60^\circ$. Peak (e) represents a second feature whose origin is very simple. In going from 2 to 3 ML, peak (e) appears strongly, and it also increases slightly in relative intensity at higher coverages. When the 90° atom is removed from the 3 ML cluster, peak (e) disappears completely, and its origin in simple forward scattering from the 90° atom(s) is thus verified. A final point concerning the peak at 45° is its sensitivity to interlayer spacing: if, for example, the *in-plane* atomic spacings are fixed at the Ni values while the *vertical* layer spacing is the 1.81 Å of Cu, a shift of this peak to 45.8° will occur.

Analogous calculations were also carried out for Cu 2p_{3/2} emission at the lower energy of 317 eV in both full clusters and clusters with atom removal. In general, although a peak at 45° and a peak at ~30° were present in both theory and experiment above 1 ML, the agreement at this energy was not as good as with the higher-energy cases. One likely reason is the greater importance of multiple scattering at this lower energy. The longer de Broglie wavelength at this energy also results in broader diffraction features, so that a greater degree of overlap occurs between various single-atom forward-scattering and diffraction features. Thus correlations between observed peaks and single atoms are not as direct for energies < 900 eV.

In conclusion, the SSC model used here provides a very good description of the peak positions and relative intensities observed in polar-scan x-ray photoelectron and Auger diffraction data from epitaxial Cu on Ni(001). For energies ≥ 900 eV, our analysis of the peak structure as the Cu coverage increases layer by layer indicates that the major peaks (c) and (e) at 45° and 90° can be simply correlated with simple forward-scattering events from atoms along the emitter-detector direction. Thus, these peaks can be used as sensitive probes of the epitaxial morphology at low coverages in the manner proposed by Egelhoff. On the other hand, the smaller peaks (b) and (d) tend to have a more complex etiology, with contributions from both simple forward scattering and first-order diffraction from other scatterers. Therefore, the simple one-to-one correspondence between these weaker features and simple forward-scattering events suggested previously^{3,4} is not possible, although such features nonetheless can be used in conjunction with SSC calculations to derive additional useful information on the structure of epitaxial overlayers. Thus, combining such high-energy polar-scan electron diffraction measurements

with SSC calculations should provide very useful information on the thickness, orientation, and atomic structure of both epitaxial overlayers and small clusters on single-crystal substrates. Such measurements are expected to be particularly sensitive in the 0–5 ML range, and to show strong peaks due to nearest-neighbor and next-nearest-neighbor forward scattering. Obtaining analogous *azimuthal-scan*

XPD data should also provide additional information on overlayer or cluster orientations about the surface normal.

We would like to thank W. F. Egelhoff for providing us with data prior to publication, and for helpful comments. We also gratefully acknowledge the support of the National Science Foundation under Grant No. CHE83-20200.

-
- ¹S. Kono, S. M. Goldberg, N. F. T. Hall, and C. S. Fadley, *Phys. Rev. Lett.* **41**, 1831 (1978); L.-G. Petersson, S. Kono, N. F. T. Hall, C. S. Fadley, and J. B. Pendry *ibid.* **42**, 1545 (1979); S. Kono, S. M. Goldberg, N. F. T. Hall, and C. S. Fadley, *Phys. Rev. B* **22**, 6085 (1980).
²C. S. Fadley, in *Progress in Surface Science*, edited by S. G. Davison (Pergamon, New York, in press).
³W. F. Egelhoff, *J. Vac. Sci. Technol. A* **2**, 350 (1984).
⁴W. F. Egelhoff, *Phys. Rev. B* **30**, 1052 (1984).

- ⁵A. Chambers and D. C. Jackson, *Philos. Mag.* **31**, 1357 (1975).
⁶P. J. Orders, R. E. Connelly, N. F. T. Hall, and C. S. Fadley, *Phys. Rev. B* **24**, 6161 (1981).
⁷B. Sinković, P. J. Orders, C. S. Fadley, R. Trehan, Z. Hussain, and J. Lecante, *Phys. Rev. B* **30**, 1833 (1984).
⁸R. Trehan and C. S. Fadley (unpublished).
⁹M. Sagurton, E. L. Bullock, and C. S. Fadley, *Phys. Rev. B* **30**, 7332 (1984).